iScience, Volume *26*

Supplemental information

N6-methyladenosine modification promotes hepatocarcinogenesis through circ-CDYL-enriched and EpCAM-positive liver tumor-initiating exosomes

Yanping Wei, Jingbo Fu, Hailing Zhang, Yan Ling, Xuewu Tang, Shuowu Liu, Miao Yu, Fuyan Liu, Guokun Zhuang, Haihua Qian, Kecheng Zhang, Pinhua Yang, Xinwei Yang, Qi Yang, Shennian Ge, Baohua Zhang, Yexiong Tan, Liang Li, and Hongyang Wang

A

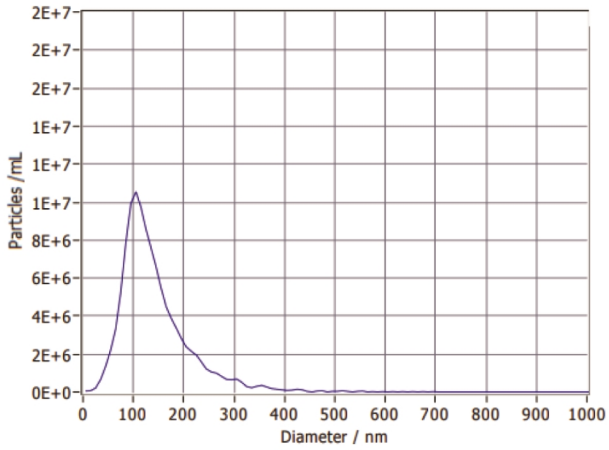

B

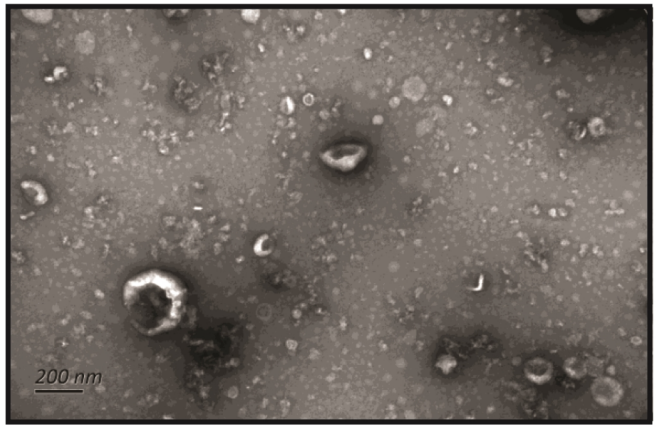

C

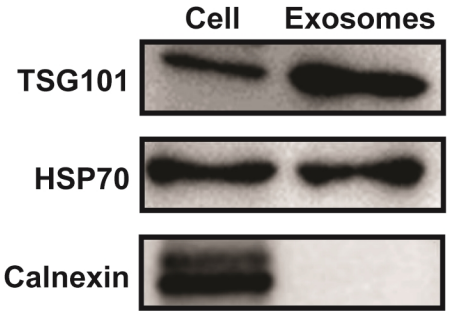

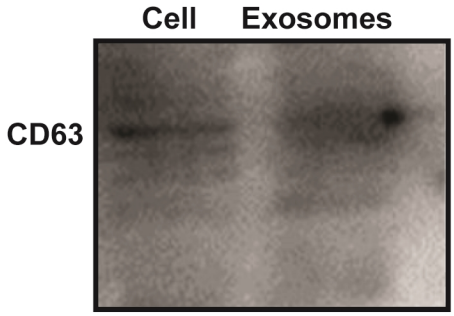

Figure S1

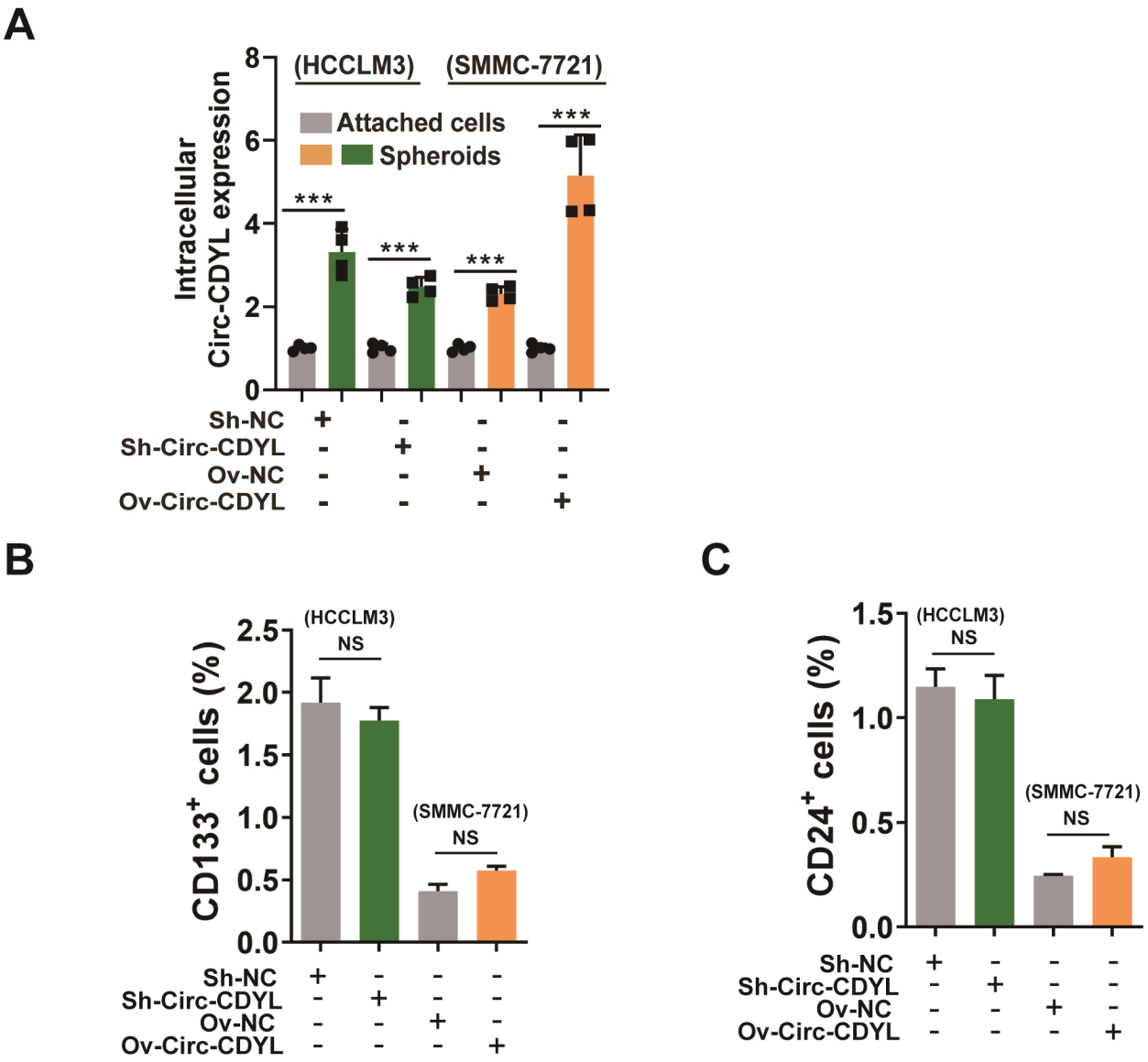
A
(HCCLM3)
(SMMC-7721)
Attached cells
Spheroids
Intracellular Circ-CDYL expression
***
Sh-NC
Sh-Circ-CDYL
Ov-NC
Ov-Circ-CDYL
B
(HCCLM3)
NS
(SMMC-7721)
NS
CD133+ cells (%)
C
CD24+ cells (%)

Figure S2

A

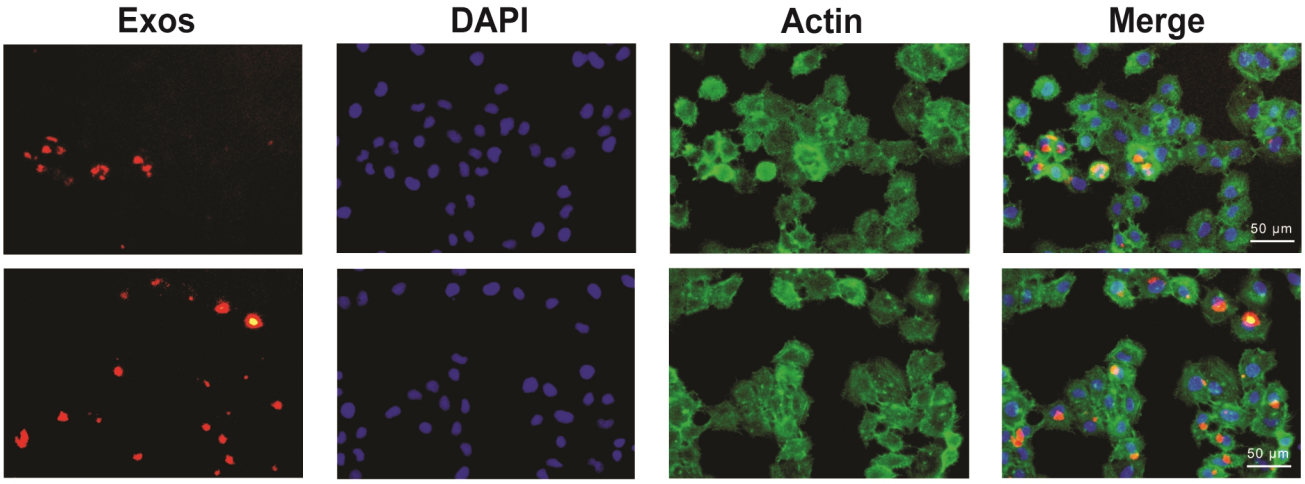

B

Frequency of colony formation		Number of cells seeded each well								T-ICs Frequency		p Value	
		500	250	125	80	40	20	10	5	Estimate	Upper and Lower Limits	Ratio Of prop.'s	Ratio of prop.'s=1
SMMC-7721	+NLTi Exo	8/8	6/8	5/8	4/8	2/8	0/8	0/8	0/8	1:151	1:97-1:235		
	+LTi Exo	8/8	8/8	8/8	7/8	5/8	3/8	3/8	2/8	1:33	1:21-1:52	0.218	0.0001

C

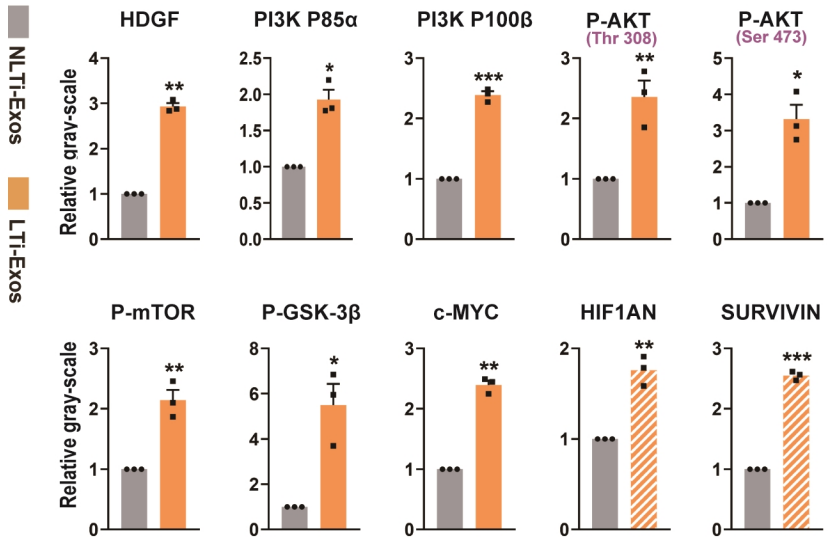

Figure S3

A

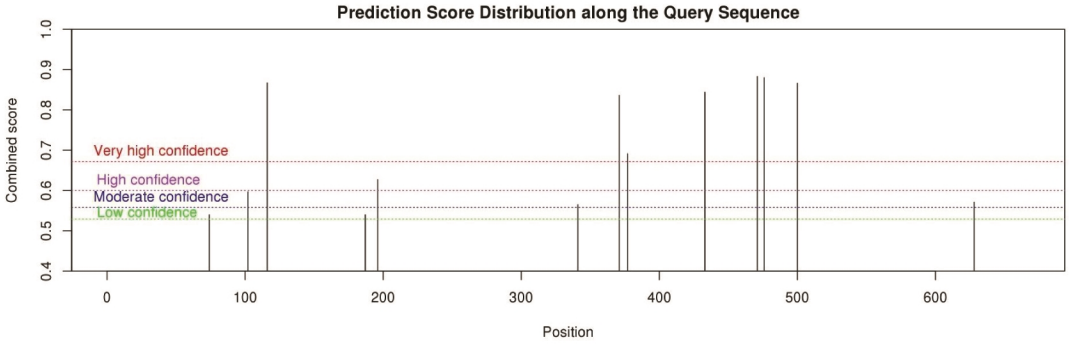

(http://www.cuilab.cn/sramp/)

B

Position	Score (binary)	Score (knn)	Score (spectrum)	Score (combined)
74	0.426	0.584	0.692	0.540
102	0.468	0.619	0.773	0.597
116	0.911	0.789	0.816	0.867
187	0.473	0.515	0.636	0.540
196	0.596	0.733	0.657	0.627
341	0.470	0.682	0.681	0.565
371	0.812	0.638	0.894	0.836
377	0.620	0.802	0.775	0.691
433	0.833	0.675	0.882	0.844
471	0.856	0.733	0.940	0.883
476	0.846	0.673	0.952	0.880
500	0.878	0.551	0.889	0.866
628	0.536	0.765	0.597	0.571

Figure S4

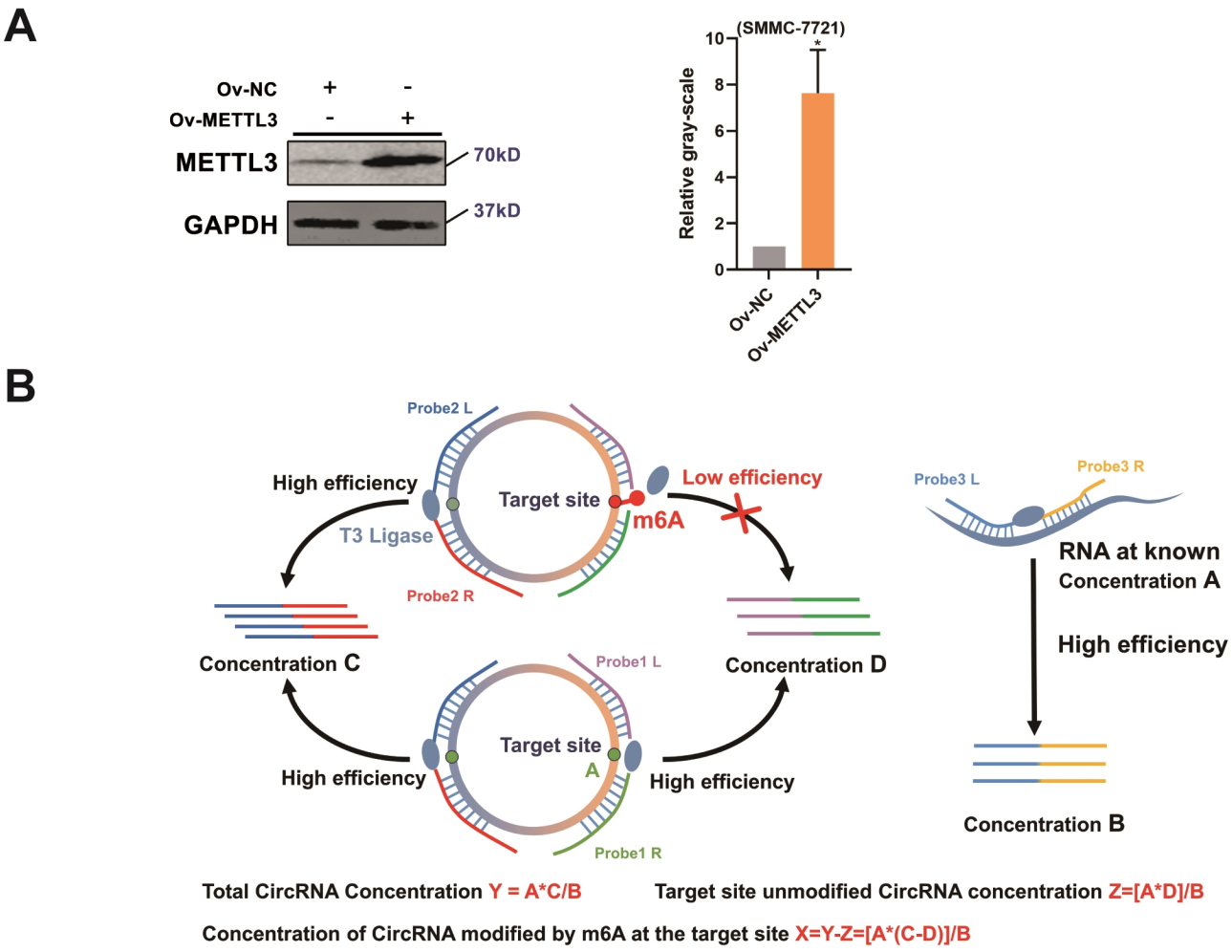

Total CircRNA Concentration Y = A*C/B Target site unmodified CircRNA concentration Z=[A*D]/B

Concentration of CircRNA modified by m6A at the target site X=Y-Z=[A*(C-D)]/B

Figure S5

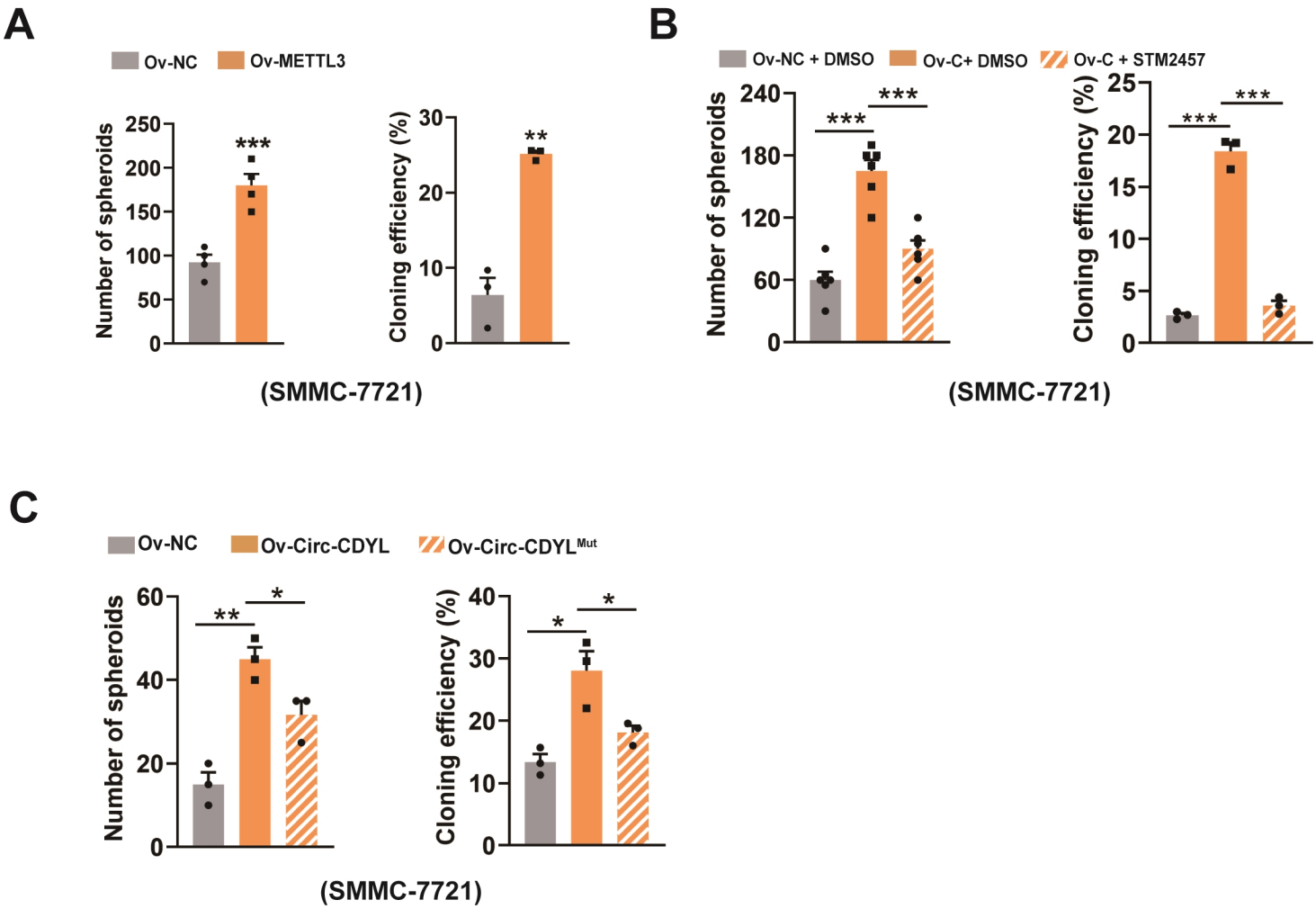
A
Ov-NC
Ov-METTL3
Number of spheroids
250
200
150
100
50
0
***
Cloning efficiency (%)
30
20
10
0
**
(SMMC-7721)
B
Ov-NC + DMSO
Ov-C+ DMSO
Ov-C + STM2457
Number of spheroids
240
180
120
60
0
***
***
Cloning efficiency (%)
25
20
15
10
5
0
***
***
(SMMC-7721)
C
Ov-NC
Ov-Circ-CDYL
Ov-Circ-CDYL Mut
Number of spheroids
60
40
20
0
**
*
Cloning efficiency (%)
40
30
20
10
0
*
*
(SMMC-7721)

Figure S6

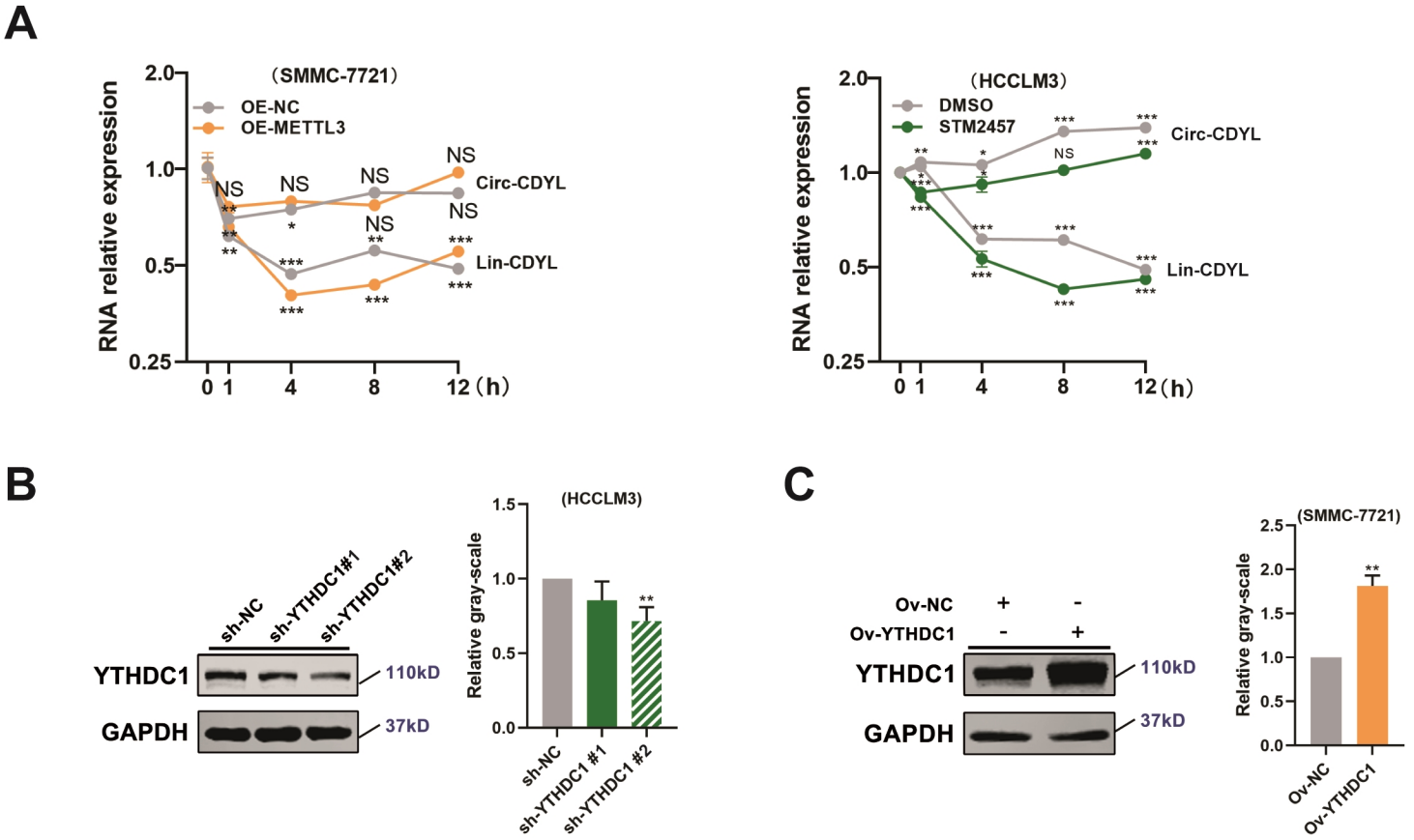
A
(SMMC-7721)
OE-NC
OE-METTL3
RNA relative expression
Circ-CDYL
Lin-CDYL
(HCCLM3)
DMSO
STM2457
0 1 4 8 12 (h)
B
sh-NC
sh-YTHDC1#1
sh-YTHDC1#2
YTHDC1
GAPDH
110kD
37kD
(HCCLM3)
Relative gray-scale
sh-YTHDC1 #1
sh-YTHDC1 #2
C
Ov-NC
Ov-YTHDC1
(SMMC-7721)
D
sh-hnRNPA2B1#1
sh-hnRNPA2B1#2
sh-hnRNPA2B1#3
hnRNPA2B1
37kD
40kD

Figure S7

Supplementary Figure Legends

Figure S1. Identification of exosomes isolated from the cell culture medium of HCC cell line, Related to Figure 1

(A) Size distribution of exosomes purified from the culture medium of HCCLM3 cells using differential ultracentrifugation methods. (B) Representative electron microscopy images of exosomes secreted from parental cells. (C) Western blot analysis of positive exosomes surface markers (TSG101, HSP70, and CD63) and a negative marker (Calnexin) on HCCLM3 cells and cell-derived exosomes, respectively.

Figure S2. Circ-CDYL did not significantly regulate the proportion of CD133- and CD24-positive cells, Related to Figure 1 and Figure 2

(A) The intracellular expression of Circ-CDYL in attached cells and spheroids cultured in low-attachment culture plates of Circ-CDYL ectopically expressed and knockdown HCC cells, as determined by RT–qPCR assay. (B-C) The percentage of $CD133^+$ cells (B) and $CD24^+$ cells (C) determined by flow cytometry in Circ-CDYL ectopically expressed and knockdown HCC cells.

Figure S3. Exosomes uptake and stemness promotion when cocultured with HCC cells, Related to Figure 2

(A) LTi-Exos were isolated from the cell supernatant of Circ-CDYL-overexpressing SMMC-7721 cells using ultracentrifugation and dyed with PKH26 (red). The recipient SMMC-7721 cells were dyed with DAPI (blue) and actin-tracker probe (green). (B) The limiting dilution assay after incubation with LTi-Exos or NLTi-Exos for 48 h. (C) The grey value of indicated Western blot

assay were calculated using Image J software.

Figure S4. Bioinformatic analysis of m6A-modified sites on Circ-CDYL, Related to Figure 3

(A) Predicted m6A-modified sites on Circ-CDYL analyzed by the SRAMP (B) Score of independent and combined tests of all predicted m6A-modified sites provided by training datasets of SRAMP. Orange highlight showed the predicted sites with combined score > 0.7.

Figure S5. Characterization of METTL3 ectopic cells and MazF-dependent relative quantification assays, Related to Figure 3

(A) Intracellular METTL3 protein expression level in METTL3-overexpressing SMMC-7721 cells determined by Western blot assay. (B) Mechanism of ligase-dependent absolute quantification of m6A-modification sites in Circ-CDYL.

Figure S6. Cloning efficiency of m6A-modification manipulated HCC cells, Related to Figure 3

(A-C) Cloning efficiency percent in METTL3 ectopic expression or negative control cells (A), Circ-CDYL overexpression cells treated with DMSO or STM2457 (B), and Circ-CDYL and Circ-CDYL with mutated m6A-modified sites ectopic expression cells (C) were calculated by the ratio of clone count: seed cell count.

Figure S7. Detection of the half-life of METTL3-modified HCC cells and characterization of YTHDC1- or hnRNPA2B1-modified cells, Related to Figure 4 and Figure 6

(A) Circ-CDYL and CDYL mRNA (Lin-CDYL) levels were determined at the indicated times after actinomycin D treatment in METTL3-overexpressing cells and STM2457-treated cells (5 μM for 48 hours). (B-C) Intracellular YTHDC1 protein expression level in YTHDC1 knockdown HCCLM3 cells (B) and YTHDC1 ectopic expression SMMC-7721 cells (C) determined by Western blot assay. (D) HnRNPA2B1 protein expression level in hnRNPA2B1 knockdown HCCLM3 cells.